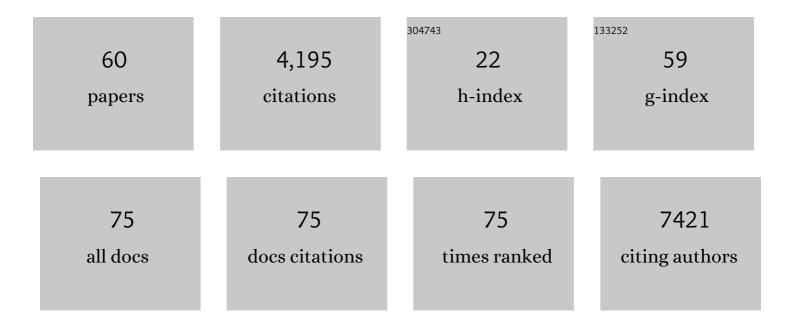
## Andrew J Logsdail

List of Publications by Year in descending order

Source: https://exaly.com/author-pdf/3485786/publications.pdf Version: 2024-02-01



#	Article	IF	CITATIONS
1	Band alignment of rutile and anatase TiO2. Nature Materials, 2013, 12, 798-801.	27.5	1,924
2	NWChem: Past, present, and future. Journal of Chemical Physics, 2020, 152, 184102.	3.0	425
3	Designer Titania-Supported Au–Pd Nanoparticles for Efficient Photocatalytic Hydrogen Production. ACS Nano, 2014, 8, 3490-3497.	14.6	279
4	Role of the Support in Gold-Containing Nanoparticles as Heterogeneous Catalysts. Chemical Reviews, 2020, 120, 3890-3938.	47.7	275
5	Polymorph Engineering of TiO <sub>2</sub> : Demonstrating How Absolute Reference Potentials Are Determined by Local Coordination. Chemistry of Materials, 2015, 27, 3844-3851.	6.7	113
6	Dopant-induced 2D–3D transition in small Au-containing clusters: DFT-global optimisation of 8-atom Au–Ag nanoalloys. Nanoscale, 2012, 4, 1109-1115.	5.6	93
7	A Selective Blocking Method To Control the Overgrowth of Pt on Au Nanorods. Journal of the American Chemical Society, 2013, 135, 6554-6561.	13.7	76
8	Deep vs shallow nature of oxygen vacancies and consequent <mml:math xmlns:mml="http://www.w3.org/1998/Math/MathML"&gt;<mml:mi>n</mml:mi>-type carrier concentrations in transparent conducting oxides. Physical Review Materials, 2018, 2, .</mml:math 	2.4	73
9	Heterogeneous Trimetallic Nanoparticles as Catalysts. Chemical Reviews, 2022, 122, 6795-6849.	47.7	61
10	Open-Source, Python-Based Redevelopment of the ChemShell Multiscale QM/MM Environment. Journal of Chemical Theory and Computation, 2019, 15, 1317-1328.	5.3	46
11	Tailoring Gold Nanoparticle Characteristics and the Impact on Aqueous-Phase Oxidation of Glycerol. ACS Catalysis, 2015, 5, 4377-4384.	11.2	45
12	Structures and Stabilities of Platinum–Gold Nanoclusters. Journal of Computational and Theoretical Nanoscience, 2009, 6, 857-866.	0.4	44
13	Embedded-cluster calculations in a numeric atomic orbital density-functional theory framework. Journal of Chemical Physics, 2014, 141, 024105.	3.0	38
14	Segregation effects on the properties of (AuAg) <sub>147</sub> . Physical Chemistry Chemical Physics, 2014, 16, 21049-21061.	2.8	37
15	Mechanistic Insight into the Framework Methylation of H-ZSM-5 for Varying Methanol Loadings and Si/Al Ratios Using First-Principles Molecular Dynamics Simulations. ACS Catalysis, 2020, 10, 8904-8915.	11.2	36
16	Bulk ionization potentials and band alignments from three-dimensional periodic calculations as demonstrated on rocksalt oxides. Physical Review B, 2014, 90, .	3.2	33
17	Morphological Features and Band Bending at Nonpolar Surfaces of ZnO. Journal of Physical Chemistry C, 2015, 119, 11598-11611.	3.1	33

Predicting the Optical Properties of Core $\hat{a}\in$  "Shell and Janus Segregated Au $\hat{a}\in$ "M Nanoparticles (M = Ag,) Tj ETQq0 Q 0 rgBT /Qyerlock 10 3.1 rgBT /Qyerlock 10 4.1 rgBT

ANDREW J LOGSDAIL

#	Article	IF	CITATIONS
19	Overgrowth of Rhodium on Gold Nanorods. Journal of Physical Chemistry C, 2012, 116, 10312-10317.	3.1	29
20	Influence of Composition and Chemical Arrangement on the Kinetic Stability of 147-Atom Au–Ag Bimetallic Nanoclusters. Journal of Physical Chemistry C, 2015, 119, 23685-23697.	3.1	29
21	Modelling metal centres, acid sites and reaction mechanisms in microporous catalysts. Faraday Discussions, 2016, 188, 235-255.	3.2	29
22	Interaction of Au16 Nanocluster with Defects in Supporting Graphite: A Density-Functional Study. Journal of Physical Chemistry C, 2011, 115, 15240-15250.	3.1	23
23	The Critical Role of βPdZn Alloy in Pd/ZnO Catalysts for the Hydrogenation of Carbon Dioxide to Methanol. ACS Catalysis, 2022, 12, 5371-5379.	11.2	23
24	Polymorphism of l â€Tryptophan. Angewandte Chemie - International Edition, 2019, 58, 18788-18792.	13.8	21
25	Computational QM/MM investigation of the adsorption of MTH active species in H-Y and H-ZSM-5. Physical Chemistry Chemical Physics, 2019, 21, 2639-2650.	2.8	21
26	Methanol loading dependent methoxylation in zeolite H-ZSM-5. Chemical Science, 2020, 11, 6805-6814.	7.4	21
27	DFT-Computed Trends in the Properties of Bimetallic Precious Metal Nanoparticles with Core@Shell Segregation. Journal of Physical Chemistry C, 2018, 122, 5721-5730.	3.1	19
28	Structural, energetic and electronic properties of (100) surfaces for alkaline earth metal oxides as calculated with hybrid density functional theory. Surface Science, 2015, 642, 58-65.	1.9	18
29	Interdependence of structure and chemical order in high symmetry (PdAu)N nanoclusters. RSC Advances, 2012, 2, 5863.	3.6	17
30	Understanding the Thermal Stability of Silver Nanoparticles Embedded in a-Si. Journal of Physical Chemistry C, 2015, 119, 23767-23773.	3.1	16
31	Development and optimization of a novel genetic algorithm for identifying nanoclusters from scanning transmission electron microscopy images. Journal of Computational Chemistry, 2012, 33, 391-400.	3.3	15
32	Controlling Structural Transitions in AuAg Nanoparticles through Precise Compositional Design. Journal of Physical Chemistry Letters, 2016, 7, 4414-4419.	4.6	15
33	Main-group test set for materials science and engineering with user-friendly graphical tools for error analysis: systematic benchmark of the numerical and intrinsic errors in state-of-the-art electronic-structure approximations. New Journal of Physics, 2019, 21, 013025.	2.9	15
34	A structure determination protocol based on combined analysis of 3D-ED data, powder XRD data, solid-state NMR data and DFT-D calculations reveals the structure of a new polymorph of <scp>l</scp> -tyrosine. Chemical Science, 2022, 13, 5277-5288.	7.4	15
35	Theoretical and Experimental Studies of the Optical Properties of Conjoined Goldâ^'Palladium Nanospheres. Journal of Physical Chemistry C, 2010, 114, 21247-21251.	3.1	14
36	Dehydrogenation and dehydration of formic acid over orthorhombic molybdenum carbide. Catalysis Today, 2022, 384-386, 197-208.	4.4	13

ANDREW J LOGSDAIL

#	Article	IF	CITATIONS
37	Hydrodeoxygenation of guaiacol over orthorhombic molybdenum carbide: a DFT and microkinetic study. Catalysis Science and Technology, 2022, 12, 843-854.	4.1	12
38	Double bubbles: a new structural motif for enhanced electron–hole separation in solids. Physical Chemistry Chemical Physics, 2014, 16, 21098-21105.	2.8	11
39	Modelling the chemistry of Mn-doped MgO for bulk and (100) surfaces. Physical Chemistry Chemical Physics, 2016, 18, 28648-28660.	2.8	11
40	QM/MM study of the reactivity of zeolite bound methoxy and carbene groups. Physical Chemistry Chemical Physics, 2021, 23, 17634-17644.	2.8	11
41	Faceting preferences for AuN and PdN nanoclusters with high-symmetry motifs. Physical Chemistry Chemical Physics, 2013, 15, 8392.	2.8	10
42	From Stable ZnO and GaN Clusters to Novel Double Bubbles and Frameworks. Inorganics, 2014, 2, 248-263.	2.7	10
43	Hybrid-DFT Modeling of Lattice and Surface Vacancies in MnO. Journal of Physical Chemistry C, 2019, 123, 8133-8144.	3.1	10
44	Coexistence of carbonyl and ether groups on oxygen-terminated (110)-oriented diamond surfaces. Communications Materials, 2022, 3, .	6.9	10
45	Polymorphism in a Multicomponent Crystal System of Trimesic Acid and <i>t</i> Butylamine. Crystal Growth and Design, 2020, 20, 5736-5744.	3.0	9
46	A quantitative multiscale perspective on primary olefin formation from methanol. Physical Chemistry Chemical Physics, 2021, 23, 21437-21469.	2.8	8
47	Solid-State Structural Properties of Alloxazine Determined from Powder XRD Data in Conjunction with DFT-D Calculations and Solid-State NMR Spectroscopy: Unraveling the Tautomeric Identity and Pathways for Tautomeric Interconversion. Crystal Growth and Design, 2022, 22, 524-534.	3.0	8
48	QM/MM study of the stability of dimethyl ether in zeolites H-ZSM-5 and H-Y. Physical Chemistry Chemical Physics, 2021, 23, 2088-2096.	2.8	7
49	Materials and Molecular Modeling at the Exascale. Computing in Science and Engineering, 2022, 24, 36-45.	1.2	7
50	A computational study of direct CO <sub>2</sub> hydrogenation to methanol on Pd surfaces. Physical Chemistry Chemical Physics, 2022, 24, 9360-9373.	2.8	7
51	Hydride Pinning Pathway in the Hydrogenation of CO <sub>2</sub> to Formic Acid on Dimeric Tin Dioxide. ChemPhysChem, 2019, 20, 680-686.	2.1	6
52	Tuning the transition barrier of H <sub>2</sub> dissociation in the hydrogenation of CO <sub>2</sub> to formic acid on Ti-doped Sn <sub>2</sub> O <sub>4</sub> clusters. Physical Chemistry Chemical Physics, 2021, 23, 204-210.	2.8	6
53	Magnetic coupling constants for MnO as calculated using hybrid density functional theory. Chemical Physics Letters, 2017, 690, 47-53.	2.6	5
54	Polymorphism of l â€∓ryptophan. Angewandte Chemie, 2019, 131, 18964-18968.	2.0	5

ANDREW J LOGSDAIL

#	Article	IF	CITATIONS
55	A combined periodic DFT and QM/MM approach to understand the radical mechanism of the catalytic production of methanol from glycerol. Faraday Discussions, 2021, 229, 108-130.	3.2	5
56	A computational study of the properties of low- and high-index Pd, Cu and Zn surfaces. Physical Chemistry Chemical Physics, 2021, 23, 14649-14661.	2.8	5
57	Improving the Adsorption of Au Atoms and Nanoparticles on Graphite via Li Intercalation. Journal of Physical Chemistry C, 2013, 117, 22683-22695.	3.1	4
58	Highlights from Faraday Discussion on Designing Nanoparticle Systems for Catalysis, London, UK, May 2018. Chemical Communications, 2018, 54, 9385-9393.	4.1	2
59	Computational investigation of CO adsorbed on Aux, Agx and (AuAg)x nanoclusters (x = 1 â^ 5, 147) and monometallic Au and Ag low-energy surfaces. European Physical Journal B, 2018, 91, 1.	1.5	1
60	Atomic Cluster Structure Identification Using Aberration-corrected Scanning Transmission Electron Microscopy. Microscopy and Microanalysis, 2012, 18, 534-535.	0.4	0